DARU Journal of Pharmaceutical Sciences (2024) 32:197–206
https://doi.org/10.1007/s40199-024-00505-2

RESEARCH ARTICLE

Activity of zinc oxide and zinc borate nanoparticles against resistant bacteria in an experimental lung cancer model

Demet Celebi[1,2] · Ozgur Celebi[3] · Ali Taghizadehghalehjoughi[4] · Sumeyye Baser[3] · Elif Aydın[5] · Daniela Calina[6] · Ekaterina Charvalos[7] · Anca Oana Docea[8] · Aristidis Tsatsakis[9] · Yaroslav Mezhuev[10,11] · Serkan Yildirim[12]

Received: 24 April 2023 / Accepted: 23 January 2024 / Published online: 17 February 2024

Abstract

Background Recent research indicates a prevalence of typical lung infections, such as pneumonia, in lung cancer patients. *Klebsiella pneumoniae*, *Pseudomonas aeruginosa*, and *Acinetobacter baumannii* stand out as antibiotic-resistant pathogens. Given this, there is a growing interest in alternative therapeutic avenues. Boron and zinc derivatives exhibit antimicrobial, antiviral, and antifungal properties.

Objectives This research aimed to establish the effectiveness of ZnO and ZB NPs in combating bacterial infections in lung cancer cell lines.

Methods Initially, this study determined the minimal inhibitory concentration (MIC) and fractional inhibitory concentration (FIC) of zinc oxide nanoparticles (ZnO NPs) and zinc borate (ZB) on chosen benchmark strains. Subsequent steps involved gauging treatment success through a lung cancer-bacteria combined culture and immunohistochemical analysis.

Results The inhibitory impact of ZnO NPs on bacteria was charted as follows: 0.97 µg/mL for *K. pneumoniae* 700603, 1.95 µg/mL for *P. aeruginosa* 27853, and 7.81 µg/mL for Acinetobacter baumannii 19,606. In comparison, the antibacterial influence of zinc borate was measured as 7.81 µg/mL for Klebsiella pneumoniae 700603 and 500 µg/mL for both *P. aeruginosa* 27853 and *A.baumannii* 19606. After 24 h, the cytotoxicity of ZnO NPs and ZB was analyzed using the MTT technique. The lowest cell viability was marked in the 500 µg/mL ZB NPs group, with a viability rate of 48.83% ($P < 0.001$). However, marked deviations appeared at ZB concentrations of 61.5 µg/mL ($P < 0.05$) and ZnO NPs at 125 µg/mL.

Conclusion A synergistic microbial inhibitory effect was observed when ZnO NP and ZB were combined against the bacteria under investigation.

Keywords *Acinetobacter baumannii* · ZnO NP · Zinc borate · *Klebsiella pneumoniae* · *Pseudomonas aeruginosa* · Lung cancer

Introduction

Lung cancer remains the leading cause of cancer-related fatalities globally [1]. Pneumonia poses a significantly heightened risk to cancer patients, resulting in higher morbidity and mortality levels than other infectious diseases [2]. Pneumonia impacts 50–70% of lung cancer patients [3]. Bacterial infections are predominantly caused by *E. coli* (44.2%), *S. aureus* (20.6%), *K. pneumoniae* (11.3%), *E. faecalis* (6.8%), *P. aeruginosa* (5.6%), *S. pneumoniae* (5.3%), *E. faecium* (4.5%), and *Acinetobacter spp*. (1.7%) [4]. Bacterial strains like *P. aeruginosa*, *K. pneumoniae*, and *A. baumanii* are responsible for hospital-acquired pneumonia; worryingly, the resistance to treatments targeting these pathogens is rising yearly [4]. *E. coli, S. aureus, S. pneumoniae*, and *K. pneumoniae* rank among the top drug-resistant bacteria. Data from the Center for Disease Control and Prevention CDC's 2019 Antibiotic Resistance report highlights the gravity of this situation, revealing that annually, the U.S. witnesses over 2.8 million antibiotic-resistant infections and more than 35,000 resultant deaths [4, 5].

Traditional antibiotic treatments, primarily composed of organic compounds, are increasingly proving ineffectual against hospital-acquired infections. For instance, in the U.S., approximately 20% of *Klebsiella* infections have shown significant resistance to third-generation cephalosporins

Extended author information available on the last page of the article

treatments [6], although they still demonstrate susceptibility to aminoglycoside antibiotics. Treating infections caused by *P. aeruginosa* and *A. baumannii* becomes even more challenging, often due to heightened multi-drug resistance. This resistance frequently emerges from genetic mutations induced by the consistent use of antibiotics [7–9]. Hence, to address these infections effectively, the pace of antibacterial drug development must match the rapid emergence of new resistant strains. Utilizing inorganic antimicrobial substances in infection management is gaining traction due to their numerous benefits over their organic counterparts, including reduced host toxicity, prolonged durability, superior stability, minimal microbial resistance, and enhanced selectivity [10]. Zinc oxide (ZnO) stands out among these inorganic agents due to its reduced cytotoxicity, heightened selectivity, and robust stability. Research indicates that smaller-sized ZnO nanoparticles (NPs) exhibit superior antimicrobial efficacy compared to their larger counterparts, positioning them as potential alternatives for treating multidrug-resistant bacteria [11–13].

Nanotechnology is rapidly emerging as a promising avenue in cancer therapeutics [14]. The intersection of nanotechnology and biology—nanobiotechnology—proposes integrating diagnostic and therapeutic modalities, which is central to a personalized approach to cancer treatment [15]. Nanoparticles serve as minuscule carriers, playing a pivotal role in diagnosing and treating an array of diseases, including cancers. Their distinctive feature of a high surface-to-volume ratio allows them to bind, adsorb, and transport minute biomolecules such as DNA, RNA, drugs, and proteins directly to specific targets, amplifying the effectiveness of therapeutic interventions [16]. Exploring antibacterial nano agents is relevant across diverse sectors like medicine, food production, textiles, packaging, and construction [17]. Metal oxide nanoparticles, in contrast to conventional compounds [18], showcase stability under harsh conditions, possess antimicrobial qualities even at minimal concentrations, and are generally deemed safe for human consumption [19]. Within metal oxide substances, ZnO emerges as a potent antibacterial contender [20]. Exhibiting various structural forms, Zinc oxide nanoparticles have demonstrated significant inhibitory effects on a broad range of bacterial species [11]. Nanomaterials' antibacterial properties predominantly stem from their large surface-to-volume ratio [11, 21] and their distinct physicochemical attributes. While the exact mechanisms remain a topic of scholarly discussion, several models have been proposed. Drawing from existing literature [11, 22–25], fundamental mechanisms include electrostatic interactions between ZnO nanoparticles (NPs) and bacterial cell walls, which compromise the cell's integrity; the release of antimicrobial Zn^{2+} ions, associated with ZnO NP accumulation in bacterial cells, leading to the formation of reactive oxygen species (ROS). Many boron-based compounds also demonstrate antiseptic properties. Boron-infused antibiotics like boromycin, aplasmomycin, and tartrolone B have shown significant activity against Gram-positive bacteria [26, 27]. However, these boron-rich antibiotics have challenges, including high costs, suboptimal bioavailability, and inefficacy against gram-negative strains. Simpler boron formulations, like boric acid and sodium tetraborate, also manifest antibacterial properties [28]. For instance, 3% boric acid application to deep-set wounds has been observed to expedite the healing process significantly, reducing hospital admissions in intensive care settings [29]. Furthermore, a hydrogel blend incorporating boron and poloxamers (F68 and F127) enhanced burn wound recovery by promoting capillary formation and fibroblast activity [30, 31]. Given the recognized antibacterial prowess of zinc oxide nanoparticles and select boron-derived molecules, our research endeavors to unearth novel nanoscale antibiotics harnessing the combined potential of zinc and boron compounds.

Methods

Chemicals and bacterial strains

For this research, we purchased zinc oxide nanoparticles and zinc borate (ZB), both with a purity level of 99%, from Sigma - Aldrich (St. Louis, MO, USA). These were prepared in line with the guidelines provided by the manufacturer. Additionally, we incorporated reference strains of *K. pneumoniae* 700603, *P. aeruginosa* 27853, and *A. baumannii* 19606, which were obtained in a lyophilized state. These strains were also prepared following the manufacturer's specified instructions.

Preparation of bacteria

The lyophilized bacteria were rehydrated by adding 1000 µl of sterile saline solution. This suspension was then inoculated into 100 µL of Tryptic Soy Broth (TSB) from Sigma–Aldrich (St. Louis, MO, USA). It was left to incubate at 37 °C for 24 h in a shaking incubator operating at 150 rpm. Following this period, the culture was plated onto Muller Hinton agar to isolate individual colonies; these plates were then incubated at 37 °C for an additional 24 h. After this interval, the growth was examined, and the proliferating colonies were selected and prepared for subsequent experiments.

Determination of antimicrobial susceptibility test with MIC

In this experiment, optimal MIC concentrations of ZnO NPs and ZB compounds were combined with the anticipation of

bacterial growth. Culturing commenced from an individual colony in a liquid medium until the determination of the minimal inhibitory concentration. Subsequently, each well received 200 µL of a glucose-fortified culture medium containing TTC (5 mg/mL) and was incubated at 37 °C for 3–4 h. Post-incubation, the depth of the red hue was deemed indicative of the viable cell count and was quantified using an ELISA reader (Biotek ELX800; BioTek Instruments, Inc.) at a wavelength of 570 nm. Results were contrasted with negative controls (absent ZnO NPs or ZB). All experiments were conducted in triplicate. The microdilution technique was utilized to identify the Minimum Inhibitory Concentration (MIC) values of ZnO NPs and ZB compounds against the bacterial strains. Concentrations ranged from 0.97 to 1024 µg/mL. Notably, the lower the antibiotic dosage, the reduced toxicity is manifested in the cell. These dosage ranges were chosen to mitigate cellular harm, t. In 180 µL quantities, each dilution was introduced into 96-well plates filled with Mueller Hinton Broth (MHB) medium. Following this, 20 µL of the microbial agent, at a concentration of 108 CFU/mL, was infused into every well, followed by a 37 °C incubation for 24 h. After this period, each well was supplemented with a water-soluble TTC salt solution, serving as a biological marker (5 mg/mL), and the plates underwent a further 2–3 h of incubation.

Fractional inhibitory concentration (FIC)

The combined effects of antimicrobial agents were assessed based on the Clinical and Laboratory Standards Institute (CLSI) guidelines and the European Antimicrobial Susceptibility Test (EUCAST). A synergistic effect is observed when the combined impact of the agents surpasses the total of their individual effects when used separately. Conversely, when the combined result mirrors the sum of the individual outcomes, it is termed an additive interaction. Adhering to the test principle, if the outcome derived from a combined drug use matches that of a single drug, it is deemed ineffective; if the combined effect is inferior to the effects of the individual drugs, it is termed antagonistic.

Σ FIC index = FIC A + FIC B
Σ FIC index $\leq$ 0.5: synergy
Σ FIC index > 0.5 and < 1: additive
Σ FIC index $\geq$ 1 and 4 $\leq$: ineffective (indifference)
Σ FIC index > 4: antagonism.

Microdilution panels

Solutions were formulated based on the predetermined panels to ascertain the final concentrations of ZnO NPs and ZB compounds. Intermediate dilutions were made at concentrations fourfold more incredible than the final desired concentration within the wells. Subsequently, each well was supplemented with 100 µL of MHB broth. Starting with ZB, a half-dilution dispersion of 100 µL was introduced, followed by another 100 µL of ZnO NPs diluted solution (with a concentration of 1024 µg/mL). Both a negative control, using just the medium, and a positive control, using bacterial wells, were set up. Excluding the negative control well, 5 µL of the antimicrobial solution was dispensed into the plates. This entire procedure was replicated thrice for ZnO NPs and ZB.

Cell cultureinfection experimental model and MTT assay

A549 cell cultures (CCL-185, ATCC) were sourced from the Medical Pharmacology Department at Bilecik Seyh Edebali University, Turkey, for this study. In brief, cells were resuspended in a refreshed medium comprising DMEM, 10% fetal bovine serum (FBS), and a 1% antibiotic blend containing penicillin, streptomycin, and amphotericin B (procured from Sigma Aldrich, St. Louis, MO, USA). Subsequently, cells were allocated in 24-well plates (provided by Corning, Inc.), in the manner previously described and were maintained in an incubator set at 5% CO_2 and 37 °C [32, 33]. The bacterial suspension was introduced to the cellular culture upon reaching a confluence level of 85% using the 0.5 McFarland standard. After 30 min, the cultures were subjected to various treatments over 24 h. Concluding the 24-hour exposure to boric acid and potassium metaborate, each well was supplemented with 10 µL of MTT solution (obtained from Sigma Aldrich, St. Louis, MO, USA) and incubated for 4 h. After that, to dissolve the Formazan crystals, each well was treated with 100 µL of DMSO (sourced from Millipore Sigma). The solutions' optical densities were assessed at a wavelength of 570 nm using the Multiskan™ GO microplate spectrophotometer (Thermo Fisher, Porto Salvo, Portugal) [32].

Immunofluorescence

A549 cell cultures were fixed with paraformaldehyde solution for 30 min, preserving the cellular structures. Cells were then treated with 3% H_2O_2 for 5 min; this step deactivates endogenous peroxidases, which can otherwise interfere with the staining procedure. The cells were treated with 0.1% Triton-X solution for 15 min. This step permeabilizes the cell membranes, facilitating the entry of antibodies into the cells. Cells were rinsed with PBS (phosphate-buffered saline) to remove any residues of the previously used chemicals. Protein blocks were applied to the cells for 5 min in darkness. Blocking solutions prevent non-specific antibody binding. The primary antibody specific for 8-OHdG (sc-66,036 from Santa Cruz Biotechnology, Texas, USA) was diluted to a

1/100 ratio and then applied to the cells. The incubation duration followed the manufacturer's recommendation. After the primary antibody incubation, the cells were treated with a fluorescently labeled secondary antibody, FITC (ab6785 from Abcam, Boston, USA), diluted to a 1/500 ratio. The samples were kept in the dark for 45 min to prevent the breakdown of the fluorescent marker. DAPI, a blue fluorescent dye that binds to DNA, was added (D1306 from Thermo Fisher, Porto Salvo, Portugal) at a 1/200 dilution ratio. The purpose of this step is to stain the cell nuclei, enabling researchers to visualize cell architecture under a fluorescence microscope; this was done for 5 min in darkness. Finally, the stained cells were sealed under a coverslip to be readied for microscopy. The stained specimens were carefully examined using a fluorescence microscope (Zeiss AXIO, Jena, Germany) to visualize the presence and distribution of 8-OHdG in the cells, indicative of oxidative DNA damage [32].

Statistical analysis

From each captured image (from the fluorescence microscope), 5 areas (ROIs) were chosen randomly. The intensity of positive staining (indicative of the presence of the marker, like 8-OHdG in this case) in these selected areas was measured using the ZEISS Zen Imaging Software. This software helps in quantifying the percentage of area that's positively stained within the selected ROIs, which essentially measures the extent of oxidative DNA damage in those regions. The percentage area values, representing the extent of positive staining, were represented as mean ± standard deviation (SD). The One-way ANOVA test was employed to determine if there were any significant differences in the staining intensities across the different groups/samples. If the ANOVA showed a significant difference, the Tukey test was used post-hoc to identify which specific groups differed from each other. A p-value (P) of less than 0.05 ($P < 0.05$) was set as the threshold for significance. In other words, if the p-value from the tests was less than 0.05, it indicated that the observed differences in staining intensities among the groups were statistically significant. The final results were presented as mean ± SD for each group, highlighting any significant differences between groups.

Results

Microbiological results

Minimal inhibitory concentration

Minimum inhibitory concentrations for standard strains were determined using the microplate method. ZnO nanoparticles demonstrated antibacterial activity at lower doses compared to ZB. Specifically, ZnO exhibited efficacy at 0.97 µg/mL against *K. pneumoniae* 700603, 1.95 µg/mL against *P. aeruginosa* 27853, and 7.81 µg/mL against *A. baumannii* 19606. Results were obtained after three replicates, and these data are summarized in Table 1.

Fractional inhibitory concentration (FIC)

Table 2 displays the synergistic, additive, antagonistic, or ineffective interactions between ZnO NPs and ZB across concentrations ranging from 500 µg/mL to 15.62 µg/mL. Notably, a synergistic effect was seen when ZnO NPs and ZB were combined at 31.25 + 62.5 µg/mL, and an additive effect was observed at 31.25 + 125 µg/mL. Other combinations yielded no significant effects. Specifically for *K. pneumoniae* 700603, the ZnO NPs + ZB combination at 31.25 + 62.5 µg/mL demonstrated a synergistic effect, while other combinations had no discernible impact. A similar synergistic effect was also noted for *P. aeruginosa* 27853 at the same concentration, with no effects seen at other concentrations. The findings related to *A. baumannii* 19,606 were consistent with the abovementioned strains. These results are detailed in Table 2.

Cell culture results

MTT test

The cytotoxic effects of ZnO NPs at concentrations of 31.2, 61.5, 125, 250, and 500 µg/mL, as well as ZB at concentrations of 31.2, 61.5, 125, 250, and 500 µg/mL, were determined after 24 h using the MTT method (Fig. 1). All data were compared to a control group with a cell viability rate of 100%. The DMSO control group did not exhibit a statistically significant difference compared to the main control group ($P > 0.05$). Viability in the groups treated with increasing doses of ZnO NP decreased, with the lowest viability observed at 500 µg/mL (viability rate of 48.83%) ($P < 0.001$). ZB exhibited more significant toxicity than ZnO NPs at equivalent doses. Notably, significant differences in

Table 1 Minimum inhibitory concentration (MIC) of ZnO NPs and zinc borate (ZB) versus standard strains

Bacteria	Antimicrobial agents	
	ZnO (µg/mL)	Zinc Borate (ZB) (µg/mL)
K. pneumoniae 700603	0.97	> 1024
P. aeruginosa 27853	1.95	7.81
A. baumannii 19606	7.81	> 1024

Table 2 FIC values of ZnO NPs + ZB on standard strains

Doses	K.pneumoniae 700603	P. aeruginosa 27853	A. baumannii 19606
ZnO NPs 500 – 15,62 µg/mL + ZB 500 µg/mL	2.22-2.0 (Ineffective)	2.45–2.11 (Ineffective)	3.1–1.91 (Ineffective)
ZnO NPs 500 – 15,62 µg/mL + ZB 250 µg/mL	2.44–1.93 (Ineffective)	2.78–1.85 (Ineffective)	3.0-1.91 (Ineffective)
ZnO NPs 500 – 15,62 µg/mL + ZB 125 µg/mL	2.21–0.6 (Ineffective) *ZnO NPs 31.25 µg/mL + ZB 125 µg/mL 0.6 (Only synergistic)	2.43–1.63 (Ineffective)	3.16–1.48 (Ineffective)
ZnO NPs 500 – 15,62 µg/mL + ZB 62,5 µg/mL	2.4 – 0.3 (Ineffective) *ZnO NPs 31.25 µg/mL + ZB 62.5 µg/mL (Only synergistic)	2.71 – 0.41 (Ineffective) *ZnO NPs 31.25 µg/mL + ZB 62.5 µg/mL (Only synergistic)	2.24–0.49 (Ineffective) *ZnO NPs 31.25 µg/mL + ZB 62.5 µg/mL (Only synergistic)
ZnO NPs 500 – 15,62 µg/mL + ZB 31,25 µg/mL	2.3–1.86 (Ineffective)	2.18–1.44 (Ineffective)	2.46–1.47 (Ineffective)
ZnO NPs 500 – 15,62 µg/mL + ZB 15,62 µg/mL	2.11–1.9 (Ineffective)	3.0-1.93 (Ineffective)	3.5–2.03 (Ineffective)

[1*]Only the synergistic agent and its value within the dilution range

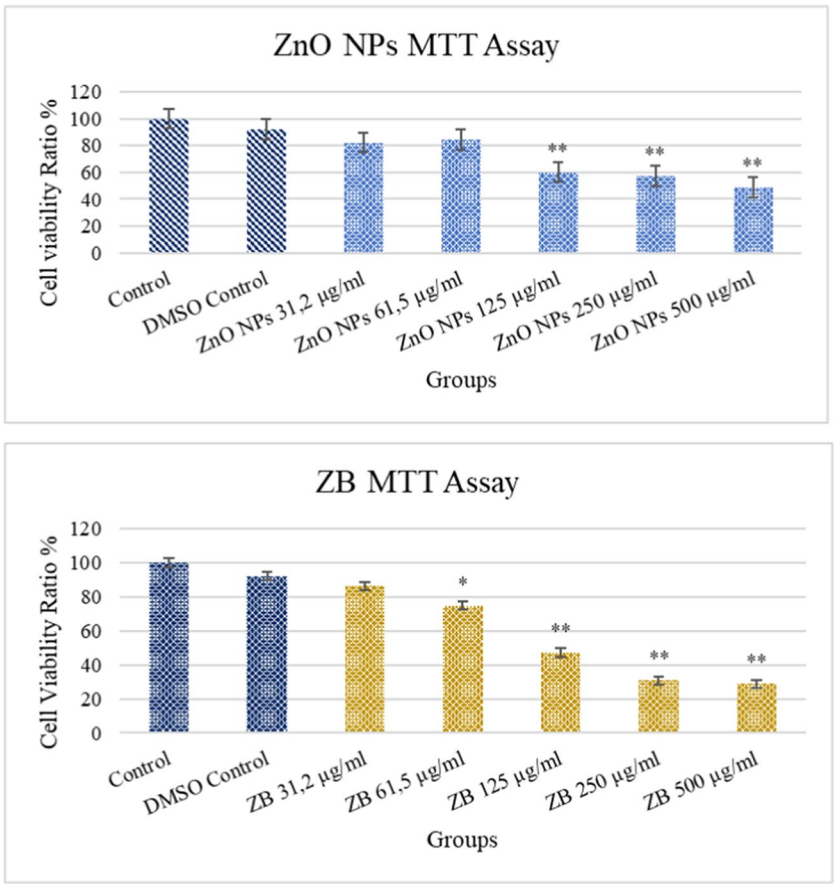

Fig. 1 Cell viability ratio of 549 cells after 24 h. The viability ratios of the ZnO NP and ZB (31.2, 61.5, 125, 250, and 500 µg/mL) groups were compared with that of the control group (*$P < 0.05$, ** $P < 0.001$)

ZB began at 61.5 µg/mL ($P < 0.05$), whereas ZnO NPs began at 125 µg/mL. The viability rate dropped sharply at 250 µg/mL, after which the decline in viability slowed ($P < 0.001$) (Fig. 1).

Immunofluorescent staining results

Control group: In the A549 cell line, 8-OHdG expression was evaluated as negative (Fig. 2). DMSO group: In the A549 cell line, 8-OHdG expression was evaluated as negative (Fig. 2). *Acinetobacter* group: Severe cytoplasmic 8-OHdG expression was detected in the A549 cells (Fig. 2). *Pseudomonas* group: Intense intracytoplasmic 8-OHdG expression was observed in A549 cells (Fig. 2). *Klebsiella* group: Intense intracytoplasmic 8-OHdG expression was observed in A549 cells (Fig. 2). Meropenem group: A very slight 8-OHdG expression was observed in A549 cells. Piperacillin-Tazobactam group: Very slight intracytoplasmic 8-OHdG expression was observed in A549 cells. Ampicillin sulbactam group: A slight cytoplasmic 8-OHdG expression was observed in A549 cells. ZnO NPs + ZB + *Acinetobacter* group: Moderate intracytoplasmic 8-OHdG expression was observed in A549 cells. A statistically significant difference ($P < 0.05$) was found compared to the Acinetobacter group. ZnO NPs + ZB + *Pseudomonas* group: Mild cytoplasmic 8-OHdG expression was observed in A549 cells. A statistically significant difference ($P < 0.05$) was found compared to the Pseudomonas group.

ZnO NPs + ZB + *Klebsiella* group: Slight cytoplasmic 8-OHdG expression was observed in A549 cells (Fig. 2). Compared to the Klebsiella group, a statistically significant difference ($P < 0.05$) was found. Analysis and statistical data from immunofluorescence results are presented in Table 3.

Discussion

Antimicrobial resistance is primarily attributed to standard drug resistance strategies such as efflux pumps, alterations at the target location, and enzymatic decomposition [34–37]. β-lactam antibiotics, encompassing penicillins, cephalosporins, and carbapenems, have historically been the choice for addressing long-standing infections by Gram-negative bacteria, especially with the growing cases of carbapenem-resistant *K. pneumoniae*. Moreover, *A. baumannii* frequently displays antibiotic resistance, presenting a significant concern in surgical areas and intensive care settings. Recently, the rise of *A. baumannii* and *E.coli* strains producing carbapenemases and harboring imipenem metallo-β and oxacillinase serine β-lactamases encoded by bla OXA has been documented. These strains exhibit resistance to both colistin and imipenem. Their amalgamation of resistance genes enables them to withstand the impact of many standard antibiotic agents. Numerous *P. aeruginosa* strains inherently exhibit diminished sensitivity to a range of antibacterial compounds and are prone to developing resistance during treatment, especially those resistant to carbapenems, primarily imipenem. The predominant mechanism underpinning imipenem resistance in P. aeruginosa intertwines chromosomal AmpC production with porin modulation. Interestingly, minimal AmpC enzyme production does not escalate carbapenem resistance due to its limited capability to break down carbapenem medications. However, when overproduced, it plays a role in intensified carbapenem resistance, especially when paired with diminished outer membrane porin permeability or amplified efflux pump activity [35, 36, 38]. Additionally, *P. aeruginosa* synthesizes ESBLs and might possess other antibiotic-resistance enzymes, including *K. pneumoniae* carbapenemases and imipenem metallo-β-lactamases like VIM. This ensemble of enzymes culminates in elevated carbapenem resistance levels in *P. aeruginosa* samples. Moreover, resistance patterns related to the rise of fluoroquinolone-resistant strains can be hosted on identical plasmids [37]. The shortcomings of traditional treatments have driven the quest for alternative solutions. Recent research outcomes suggest a reduction in treatment side effects and a burgeoning interest in nanoparticles known for their minimized cytotoxic impacts. The medical sector has witnessed an uptick in the application of nanoparticles, which can influence the metabolism of multiple pathogenic bacteria directly or indirectly. Beyond their reduced toxicity and favorable biological properties, ZnO-NPs also exhibit antimicrobial and anticancer activities [25]. Research exploring the antibacterial efficacy of nanoparticles against respiratory pathogens revealed that ZnO-NPs demonstrated superior activity against gram-negative bacteria. This study also underscored that nanoparticles displayed low MICs for these Gram-negative bacteria [39]. Separate research has highlighted the potent antimicrobial prowess of ZnO NPs among inorganic antimicrobials attributed to the significant oxidative destruction from reactive oxygen species [40–42]. Our investigation quantified the potency of the individual nano molecule ZnO NPs against *K. pneumoniae* 700603 at 0.97 µg/mL, P. *aeruginosa* 27853 at 1.95 µg/mL, and *A. baumannii* 19606 at 7.81 µg/mL. The MIC concentration of ZB most effective against *P.aeruginosa* 27853 was 7.81 µg/mL.

Azizi-Lalabadi et al. demonstrated a synergistic effect between ZnO NPs and Titanium dioxide (TiO_2) in their study [42]. Similarly, another research identified synergistic and additive effects of zinc oxide nanoparticles, with no observed antagonistic effects [43]. Our research detected the most pronounced synergistic effect at a fractional inhibitory concentration of ZnO NPs + ZB (31.25 + 62.5 µg/mL). Regarding the toxicity of NPs on A549 cells, one study indicated a reduction in cell viability to approximately 30% [44]. Another investigation contrasted the toxicity of ZnO and

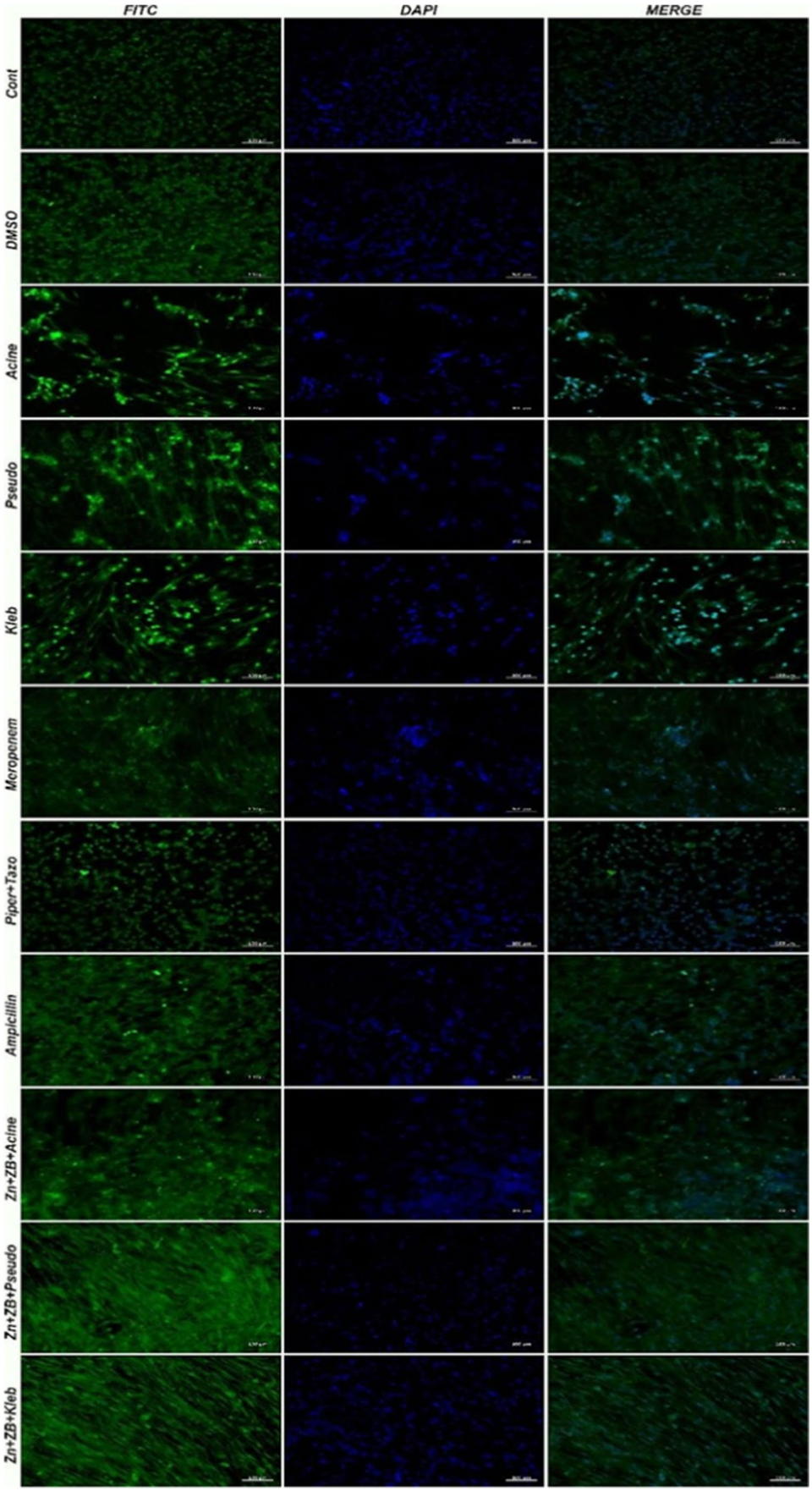

Fig. 2 Cell culture, 8-OHdG expression (FITC) and D-IF, 4',6-Diamidino-2-Phenylindole (DAPI), Bar: 100 µm

Table 3 Analysis and statistical data of immunofluorescence results in cell culture

	8-OHdG expression levels
Control	17.54 ± 0.36^{a}
DMSO 9	18.22 ± 0.51^{a}
Acinetobacter	92.59 ± 1.05^{b}
Pseudomonas	91.29 ± 1.75^{b}
Klebsiella	93.66 ± 1.87^{b}
Meropenem	25.16 ± 0.63^{c}
Piperacillin-Tazobactam	24.81 ± 1^{c}
Ampicillin Sulbactam	24.92 ± 0.48^{c}
ZnO NPs + ZB + Acinetobacter	36.19 ± 1.45^{d}
ZnO NPs + ZB + Pseudomonas	35.29 ± 1.33^{d}
ZnO NPs + ZB + Klebsiella	37.57 ± 1.44^{d}

[1a, b, c, d]different letters on the same line represent statistically significant differences ($P < 0.05$)

TiO_2 nanoparticles to A549 cells, concluding that ZnO nanoparticles were notably more lethal than TiO_2 [45]. In our research, we observed that the combined cytotoxic effects of ZnO NPs and ZB were more pronounced than that of either ZB or ZnO NPs alone, with ZnO NPs diminishing the viability of A549 cells by approximately 52%. The outcomes of this study hold promise, particularly given the low effective concentrations achieved and in light of the global challenges posed by antibiotic resistance.

Conclusion

Nanoparticles of zinc oxide and zinc borate have been shown to possess a synergistic antibacterial effect against common hospital pathogens, such as *K. pneumoniae* 700603 and *P. aeruginosa* 27853 when co-administered at concentrations of 31.25 µg/mL and 62.5 µg/mL. Additionally, zinc oxide nanoparticles display cytotoxic effects on A549 cells. This combined antibacterial and cytotoxic activity offers potential in treating patients with lung cancer further complicated by pneumonia. The synergistic antibacterial action of these nanoparticles presents a novel approach to address antibiotic-resistant strains responsible for hard-to-treat pneumonia, often resistant to conventional antibiotics. Thus, the combined use of zinc oxide and zinc borate nanoparticles emerges as a promising therapeutic avenue due to their synergistic antibacterial properties and notable antitumor activity. However, further in vivo studies are needed to assess the genotoxicity, excretion rates, and optimal methods of administering these nanoparticles to the body.

Funding This research received no external funding.

Data availability Are ready when it is needed.

Declarations

Submissions that do not include relevant declarations will be returned as incomplete.

Ethical approval No ethical permission is required for the study.

Informed consent Not applicable.

Conflict of interest On behalf of all authors, the corresponding author states that there is no conflict of interest.

References

1. Bray F, Ferlay J, Soerjomataram I, Siegel RL, Torre LA, Jemal A. Global cancer statistics 2018: GLOBOCAN estimates of incidence and mortality worldwide for 36 cancers in 185 countries. CA Cancer J Clin. 2018;68(6):394–424. https://doi.org/10.3322/caac.21492.
2. Akinosoglou KS, Karkoulias K, Marangos M. Infectious complications in patients with lung cancer. Eur Rev Med Pharmacol Sci. 2013;17(1):8–18.
3. Valvani A, Martin A, Devarajan A, Chandy D. Postobstructive pneumonia in lung cancer. Ann Transl Med. 2019;7(15):357.
4. European Centre for Disease Prevention and Control Antimicrobial resistance in the EU/EEA (EARS-Net). Annual Epidemiological Report 2019. Trop Doct. 2020;30:114–6.
5. Global antimicrobial resistance surveillance system (GLASS) report: early implementation 2020. Geneva: World Health Organization; 2020. Licence: CC BY-NC-SA 3.0 IGO.
6. Paterson DL. Resistance in gram-negative bacteria: Enterobacteriaceae. Am J Infect Control. 2006;34(5):20–8. https://doi.org/10.1016/j.ajic.2006.05.238.
7. Pang Z, Raudonis R, Glick BR, Lin TJ, Cheng Z. Antibiotic resistance in *Pseudomonas aeruginosa*: mechanisms and alternative therapeutic strategies. Biotechnol Adv. 2019;37(1):177–92. https://doi.org/10.1016/j.biotechadv.2018.11.013.
8. Laborda P, Hernando-Amado S, Martínez JL, Sanz-García F. Antibiotic resistance in pseudomonas. Adv Exp Med Biol. 2022;1386:117–43. https://doi.org/10.1007/978-3-031-08491-1_5.
9. Gordon NC, Wareham DW. Multidrug-resistant *Acinetobacter baumannii*: mechanisms of virulence and resistance. Int J Antimicrob Agents. 2010;35(3):219–26. https://doi.org/10.1016/j.ijantimicag.2009.10.024.
10. da Silva BL, Caetano BL, Chiari-Andréo BG, Pietro RCLR, Chiavacci LA. Increased antibacterial activity of ZnO nanoparticles: influence of size and surface modification. Colloids Surf B. 2019;177:440–7.
11. Sirelkhatim A, Mahmud S, Seeni A, Kaus NHM, Ann LC, Bakhori SKM, Hasan H, Mohamad D. Review on Zinc Oxide nanoparticles: antibacterial activity and toxicity mechanism. Nanomicro Lett. 2015;7(3):219–42.
12. Adeniji OO, Ojemaye MO, Okoh AI. Antibacterial activity of metallic nanoparticles against multidrug-resistant pathogens isolated from environmental samples: nanoparticles/antibiotic combination therapy and cytotoxicity study. ACS Appl Bio Mater. 2022;5(10):4814–26.

13. Riahi S, Moussa NB, Lajnef M, Jebari N, Dabek A, Chtourou R, ..., Herth E. Bactericidal activity of ZnO nanoparticles against multidrug-resistant bacteria. J Mol Liq. 2023;122596.
14. Mosleh-Shirazi S, Abbasi M, Moaddeli MR, Vaez A, Shafiee M, Kasaee SR, Amani AM, Hatam S. Nanotechnology advances in the detection and treatment of cancer: an overview. Nanotheranostics. 2022;6(4):400–23. https://doi.org/10.7150/ntno.74613.
15. Chaturvedi VK, Singh A, Singh VK, Singh MP. Cancer nanotechnology: a new revolution for cancer diagnosis and therapy. Curr Drug Metab. 2019;20(6):416–92. https://doi.org/10.2174/1389200219666180918111528.
16. Zaimy MA, Saffarzadeh N, Mohammadi A, Pourghadamyari H, Izadi P, Sarli A, et al. New methods in the diagnosis of cancer and gene therapy of cancer based on nanoparticles. Cancer GeneTher. 2017;24(6):233–43. https://doi.org/10.1038/cgt.2017.16.
17. Li Q, Mahendra S, Lyon DY, Brunet L, Liga MV, Li D, et al. Antimicrobial nanomaterials for water disinfection and microbial control: potential applications and implications. Water Res. 2008;42(18):4591–602. https://doi.org/10.1016/j.watres.2008.08.015.
18. Gao X, Yu Z, Tang X, Zhang H, Peng L, Li J. Augmented antibacterial mechanism of ZnO nanoparticles by labyrinthian-channel configuration of maize-stalk carbohydrate columns and sustainable strategy for water decontamination. J Hazard Mater. 2022;15(436):129258. https://doi.org/10.1016/j.jhazmat.2022.129258.
19. Zhu X, Wang J, Cai L, Wu Y, Ji M, Jiang H, Chen J. Dissection of the antibacterial mechanism of zinc oxide nanoparticles with manipulable nanoscale morphologies. J Hazard Mater. 2022;15(430): 128436. https://doi.org/10.1016/j.jhazmat.2022.128436.
20. He M, Li X, Yu L, Deng S, Gu N, Li L, Jia J, Li B. Double-sided Nano-ZnO: superior antibacterial properties and induced hepatotoxicity in Zebrafish Embryos. Toxics. 2022;10(3):144. https://doi.org/10.3390/toxics10030144.
21. Yılmaz GE, Göktürk I, Ovezova M, Yılmaz F, Kılıç S, Denizli A. Antimicrobial nanomaterials: a review. Hygiene. 2023;3(3):269–90. https://doi.org/10.3390/hygiene3030020.
22. Guan G, Zhang L, Zhu J, Wu H, Li W, Sun Q. Antibacterial properties and mechanism of biopolymer-based films functionalized by CuO/ZnO nanoparticles against *Escherichia coli* and *Staphylococcus aureus*. J Hazard Mater. 2021;15(402):123542. https://doi.org/10.1016/j.jhazmat.2020.123542.
23. Rayyif SMI, Mohammed HB, Curuțiu C, Bîrcă AC, Grumezescu AM, et al. ZnO Nanoparticles-Modified Dressings to Inhibit Wound Pathogens. Materials (Basel). 2021;14(11):3084. https://doi.org/10.3390/ma14113084.
24. Mendes CR, Dilarri G, Forsan CF, Sapata VMR, Lopes PRM, de Moraes PB, Montagnolli RN, Ferreira H, Bidoia ED. Antibacterial action and target mechanisms of zinc oxide nanoparticles against bacterial pathogens. Sci Rep. 2022;12(1):2658. https://doi.org/10.1038/s41598-022-06657-y.
25. Li Y, Yang Y, Qing Y, Li R, Tang X, Guo D, Qin Y. Enhancing ZnO-NP Antibacterial and Osteogenesis Properties in Orthopedic Applications: A Review. Int J Nanomedicine. 2020;20(15):6247–62. https://doi.org/10.2147/IJN.S262876.
26. Irschik H, Schummer D, Gerth K, Höfle G, Reichenbach H. The tartrolons, newboron-containing antibiotics from a myxobacterium, Sorangium cellulosum. J Antibiot. 1995;48(1):26–30. https://doi.org/10.7164/antibiotics.48.26.
27. Shimizu Y, Ogasawara Y, Matsumoto A, Dairi T. Aplasmomycin and boromycin are specific inhibitors of the futalosine pathway. J Antibiot. 2018;11:968–70. https://doi.org/10.1038/s41429-018-0087-2.
28. Yilmaz MT. Minimum inhibitory and minimum bactericidal concentrations of boron compounds against several bacterial strains. Turk J Med Sci. 2012;42:1423–9. https://doi.org/10.3906/sag-1205-83.
29. Blech M, Martin C, Borrelly J, Hartemann P. Treatment of deep wounds with loss of tissue. Value of a 3% boric acid solution. Presse Med. 1990;19(22):1050–2.
30. Doğan A, Demirci S, Çağlayan AB, Kılıç E, Günal MY, Uslu Ü, et al. Sodium pentaborate pentahydrate and pluronic containing hydrogel increases cutaneous wound healing in vitro and in vivo. Biol Trace Elem Res. 2014;162:72–9. https://doi.org/10.1007/s12011-014-0104-7.
31. Demirci S, Doğan A, Karakuş E, Halıcı Z, Topçu A, Demirci E, et al. Boron and poloxamer (F68 and F127) containing hydrogel formulation for burn wound healing. Biol Trace Elem Res. 2015;168:169–80. https://doi.org/10.1007/s12011-015-0338-z.
32. Celebi D, Taghizadehghalehjough A, Baser S, Genc S, Yilmaz A, Yeni Y, et al. Effects of boric acid and potassium metaborate on cytokine levels and redox stress parameters in a wound model infected with methicillin resistant *Staphylococcus aureus*. Mol Med Rep. 2022;26:294. https://doi.org/10.3892/mmr.2022.12809.
33. Celebi O, Celebi D, Baser S, et al. Antibacterial activity of Boron compounds against Biofilm-forming pathogens. Biol Trace Elem Res. 2023;202:346–59. https://doi.org/10.1007/s12011-023-03768-z.
34. Biendo M, Laurans G, Lefebvre JF, Daoudi F, Eb F. Epidemiological study of an *Acinetobacter baumannii* outbreak by using a combination of antibiotyping and ribotyping. J Clin Microbiol. 1999;37(7):2170–5. https://doi.org/10.1128/jcm.37.7.2170-2175.1999.
35. Fukuoka T, Ohya S, Narita T, Katsuta M, Iijima M, Masuda N. Activity of the carbapenem panipenem and role of the OprD (D2) protein in its diffusion through the *Pseudomonas aeruginosa* outer membrane. Antimicrob Agents Chemother. 1993;37(2):322–7. https://doi.org/10.1128/AAC.37.2.322.
36. Elsner HA, Sobottka I, Mack D, Claussen M, Laufs R, Wirth R. Virulence factors of *Enterococcus faecalis* and *Enterococcus faecium* blood culture isolates. Eur J Clin Microbiol Infect Dis. 2000;19(1):39–42. https://doi.org/10.1007/s100960050007.
37. Bush K, Jacoby GA, Medeiros AA. A functional classification scheme for β-lactamases and its correlation with molecular structure. Antimicrob Agents Chemother. 1995;39(6):1211–33. https://doi.org/10.1128/AAC.39.6.1211.
38. Celebi D, Aydın E, Rakici E, et al. Evaluation of presence of clone ST131 and biofilm formation in ESBL producing and non-producing Escherichia coli strains. Mol Biol Rep. 2023;50:5949–56. https://doi.org/10.1007/s11033-023-08532-z.
39. Huang YS, Wang JT, Tai HM, Chang PC, Huang HC, Yang PC. Metal nanoparticles and nanoparticle composites are effective against Haemophilus influenzae, *Streptococcus pneumoniae*, and multidrug-resistant bacteria. J Microbiol Immunol Infect. 2022;55(4):708–15. https://doi.org/10.1016/j.jmii.2022.05.003.
40. Maruthapandi M, Saravanan A, Das P, Natan M, Jacobi G, Banin E, et al. Antimicrobial activities of Zn-Doped CuO microparticles decorated on polydopamine against sensitive and antibiotic-resistant Bacteria. ACS Appl Polym Mater. 2020;2:5878–88. https://doi.org/10.1021/acsapm.0c01104.
41. Zubair N, Akhtar K. Morphology controlled synthesis of ZnO nanoparticles for InVitro evaluation of antibacterial activity. Trans Nonferrous Met Soc China. 2020;30:1605–14.
42. Azizi-Lalabadi M, Ehsani A, Divband B, Alizadeh-Sani M. Antimicrobial activity of Titanium dioxide and zinc oxide nanoparticles supported in 4A zeolite and evaluation the morphological characteristic. Sci Rep. 2019;25(1):17439. https://doi.org/10.1038/s41598-019-54025-0.

43. Sharma N, Jandaik S, Kumar S. Synergistic activity of doped zinc oxide nanoparticles with antibiotics: ciprofloxacin, ampicillin, fluconazole and amphotericin B against pathogenic microorganisms. An Acad Bras Cienc. 2016;88(3):1689–98. https://doi.org/10.1590/0001-3765201620150713.
44. He T, Long J, Li J, Liu L, Cao Y. Toxicity of ZnO nanoparticles (NPs) to A549 cells and A549 epithelium in vitro: interactions with dipalmitoyl phosphatidylcholine (DPPC). Environ Toxicol Pharmacol. 2017;56:233–40. https://doi.org/10.1016/j.etap.2017.10.002.
45. Martin A, Sarkar A. Epithelial to mesenchymal transition, eIF2α phosphorylation and Hsp70 expression enable greater tolerance in A549 cells to TiO_2 over ZnO nanoparticles. Sci Rep. 2019;24(1):436. https://doi.org/10.1038/s41598-018-36716-2.

Authors and Affiliations

Demet Celebi[1,2] · Ozgur Celebi[3] · Ali Taghizadehghalehjoughi[4] · Sumeyye Baser[3] · Elif Aydın[5] · Daniela Calina[6] · Ekaterina Charvalos[7] · Anca Oana Docea[8] · Aristidis Tsatsakis[9] · Yaroslav Mezhuev[10,11] · Serkan Yildirim[12]

✉ Aristidis Tsatsakis
tsatsaka@uoc.gr

Demet Celebi
dmtdl2006@gmail.com

Ozgur Celebi
ozgur.celebi@atauni.edu.tr

Ali Taghizadehghalehjoughi
ali.tgzd@bilecik.edu.tr

Sumeyye Baser
sumeyyebaser06@gmail.com

Elif Aydın
elif.aydin@ksbu.edu.tr

Daniela Calina
calinadaniela@gmail.com

Ekaterina Charvalos
directorcentralabs@iaso.gr

Anca Oana Docea
daoana00@gmail.com

Yaroslav Mezhuev
valsorja@mail.ru

Serkan Yildirim
srkn_yldrm25@hotmail.com

[1] Faculty of Veterinary Medicine, Department of Microbiology, Ataturk University, Ataturk University Avenue, Erzurum 25240, Turkey

[2] Vaccine Application and Development Center, Ataturk University, Ataturk University Avenue, Erzurum 25240, Turkey

[3] Faculty of Medicine, Department of Medical Microbiology, Ataturk University, Ataturk University Avenue, Erzurum 25240, Turkey

[4] Faculty of Medicine, Department of Medical Pharmacology, Seyh Edebali University, 27 Fatih Sultan Mehmet Avenue, Bilecik 11000, Turkey

[5] Tavsanli Vocational School of Health Services, Kutahya Health Sciences University, Sehit Ali Gaffar Okan Avenue, Kutahya 430200, Turkey

[6] Department of Clinical Pharmacy, University of Medicine and Pharmacy of Craiova, Craiova 200349, Romania

[7] In Vitro Labs S.A., Leventi 9, Peristeri 12132, Greece

[8] Department of Toxicology, University of Medicine and Pharmacy of Craiova, Craiova 200349, Romania

[9] Department of Forensic Sciences and Toxicology, Faculty of Medicine, University of Crete, Heraklion 71003, Greece

[10] Department of Biomaterials, Mendeleev University of Chemical Technology of Russia, 9 Miusskaya Square, Moscow 125047, Russia

[11] Laboratory of Heterochain Polymers, A. N. Nesmeyanov Institute of Organoelement Compounds, Russian Academy of Sciences, 28 Vavilova st, Moscow 119991, Russia

[12] Faculty of Veterinary Medicine, Department of Pathology, Ataturk University, Ataturk University Avenue, Erzurum 25240, Turkey